

## Fabrication of Polymeric Nanoparticles of Poly(ethylene-co-vinyl acetate) Coated with Chitosan for Pulmonary Delivery of Carvedilol

Jaleh Varshosaz,<sup>1</sup> Somaih Taymouri,<sup>1</sup> Hamed Hamishehkar<sup>2</sup>

<sup>1</sup>Department of Pharmaceutics, School of Pharmacy and Novel Drug Delivery Systems Research Centre, Isfahan University of Medical Sciences, Isfahan, Iran

<sup>2</sup>Tabriz University of Medical Sciences, Drug Applied Research Center, Tabriz, Iran

Correspondence to: J. Varshosaz (E-mail: varshosaz@pharm.mui.ac.ir)

**ABSTRACT:** Carvedilol is a drug with low oral bioavailability due to its high first-pass metabolism. The purpose of the present study was to prepare a mucoadhesive dry powder inhaler of this drug loaded in poly(ethylene-co-vinyl acetate)(PEVA) nanoparticles for pulmonary delivery. PEVA nanoparticles were prepared by an O/W solvent evaporation method and coated with different concentrations of chitosan as a mucoadhesive polymer. Encapsulation efficiency, particle size, zeta potential, release efficiency, and mucoadhesive properties of the different formulations were evaluated on mucin substrate. The optimized formulation of nanoparticles was spray dried using lactose and mannitol as carrier powders. The flowability of the obtained powders was checked by Carr's Index and Hausner ratio and the *in vitro* deposition of the aerosolized drug was investigated using a Next Generation Impactor. Increasing in the particle size and zeta potential of nanoparticles confirmed the settling of the chitosan coating layer on the surface of nanoparticles. The *in vitro* drug release from coated nanoparticles decreased with increasing of chitosan concentration. Mucoadhesive property of chitosan-coated PEVA nanoparticles was higher than noncoated ones. Spray-dried powders had different aerosolization behavior. Mannitol-based formulation was found to have low density, better flow ability, smaller aerodynamic diameter ( $d_{aer}$ ) and higher fine powder fraction. The results of the present study allow concluding that mannitol spray dried, mucoadhesive nanoparticles of PEVA are suitable inhaler powder for pulmonary delivery of carvedilol. © 2013 Wiley Periodicals, Inc. *J. Appl. Polym. Sci.* 000: 000–000, 2013

**KEYWORDS:** drug delivery systems; nanostructured polymers; nanoparticles; applications

Received 29 March 2013; accepted 18 June 2013; Published online

DOI: 10.1002/app.39694

### INTRODUCTION

Pulmonary drug delivery is a needle-free route for systemic delivery of small molecule drugs such as therapeutic peptides and proteins. The lungs are suitable site for absorption of drugs because of: (i) the large surface area of the alveoli (100 m<sup>2</sup>) immediately accessible to drug; (ii) a relatively low metabolic activity locally and lack of first-pass hepatic metabolism; and (iii) the elevated blood flow (5 L/min) which rapidly distributes molecules throughout the body.<sup>1</sup>

Carvedilol is an antihypertensive drug and its bioavailability is limited (approximately 20%) due to its first-pass metabolism.<sup>2</sup> The oral bioavailability of carvedilol was improved by drug-loaded solid lipid nanoparticles that were developed using monoglycerides as lipid and soya lecithin and Poloxamer 188 as surfactants. These nanoparticles were surface modified with a chitosan derivative, *N*-carboxymethyl chitosan for enhancing its bioavailability.<sup>2</sup> To improve carvedilol bioavailability it was also incorporated into self-nanoemulsifying drug-delivery systems composed of different ratios of polyoxyl-40 hydrogenated castor

oil, medium-chain triglycerides, and diethylene glycol monoethyl ether<sup>3,4</sup> used chitosan mucoadhesive microspheres of carvedilol for nasal delivery of this drug with enhanced bioavailability for treatment of hypertension and angina pectoris.

Nano carrier systems in pulmonary drug delivery are promising approach because of their potential to uniform distribution of drug dose among the alveoli; enhanced solubility of the drug compared to its own aqueous solubility, the sustained-release of drug which consequently reduces the dosing frequency, suitability for delivery of macromolecules and decreased incidence of side effects.<sup>5</sup> Chitosan is a polysaccharide that obtains by the alkaline deacetylation of chitin. The safety and acceptability characteristics of chitosan have facilitated its application in drug delivery by different administration routes. Chitosan is an attractive option for designing satisfactory novel drug-delivery system to be administered to or through the lungs because of its biocompatibility, biodegradability, antimicrobial, and antioxidant activities. In addition chitosan is a cationic mucoadhesive polymer with ability to establish ionic, hydrogen, and

hydrophobic bonding with negatively charged chains of mucin. These interactions increase lung retention of chitosan drug carriers.<sup>6</sup> Also chitosan can enhance absorption of drugs by the paracellular route due to the transiently disruption of tight junctions.<sup>7</sup>

Nebulizers, metered dose inhalers (MDIs), and dry powder inhalers (DPIs) are the most popular aerosol devices that are used for inhalation of drug formulations. MDIs and DPIs are commonly used because they are portable and more cost-effective than nebulizers. DPIs have some advantages including: they are propellant free and the inhalation of drugs through DPIs is controlled by respiratory effort, and the emission of drugs is actually coordinated with the breath. This, in turn, overcomes the synchronization problems associated with MDIs. So it is a good alternative device for pulmonary drug delivery.<sup>1</sup> Poly(ethylene-co-vinyl acetate) (PEVA) is a biocompatible copolymer used to deliver drugs at therapeutic levels over extended periods of time.<sup>8</sup> This polymer is added to many nanocomposites to reduce drug release rate.<sup>9–13</sup> It can provide a constant release for a period of time. Tallury et al.<sup>14</sup> used this polymer to deliver chlorhexidine and acyclovir for sustained release of drug in an extended period of time. In addition Shin and Lee<sup>15</sup> designed a transdermal patch system by PEVA for controlled release of triprolidine. Vasudev et al.<sup>16</sup> used a co-matrix of this polymer with chitosan to develop prolonged release form of aspirin and heparin as coagulant agents.

In the present study to enhance the bioavailability of carvedilol we used PEVA as a biocompatible copolymer to produce nanoparticles loaded with this drug and then the nanoparticles were coated by chitosan for designing mucoadhesive nanoparticles to prepare suitable DPI pulmonary delivery of carvedilol. To our knowledge there is no report on the fabrication of nanoparticles of PEVA nanoparticles coated with chitosan. Carvedilol is a weak base and its *pKa* value is approximately 7.8, which satisfies the criterion for the selection of the drug. The log *PC* (partition coefficient) value for carvedilol is about 2.79 (17). It indicates that carvedilol has sufficient lipophilicity to pass through the pulmonary membranes.

## MATERIALS AND METHODS

### Material

Carvedilol was received as a gift from Daru Pakhash Pharmaceutical Company (Iran), chitosan ( $M_w = 150,000$ , with the degree of deacetylation of 86.8%) was purchased from Fluka (Switzerland), lactose and mannitol were from Merck Chemical Company (Germany), PEVA (vinyl acetate 12 wt %) was supplied by (Aldrich, USA). All other chemicals and reagents used were of analytical grade and used as received.

### Preparation of PEVA Nanoparticles by Emulsion Solvent Evaporation Method

PEVA nanoparticles were prepared by O/W solvent evaporation method. Briefly, 36 mg of PEVA was dissolved in 3 mL of carbon tetrachloride. An amount of 16.8 mg carvedilol and 5.5  $\mu\text{L}$  of PEG400 were dissolved in 1.3 mL of dichloromethane (DCM). Then the two solutions were added to each other and subsequently the oil mixture was dispersed into 25 mL of an

aqueous phase containing Tween 20 (0.5% w/v). The mixture was agitated with a magnetic stirrer until the complete evaporation of organic solvent was accomplished.

### Scanning Electron Microscopy Studies

Morphology of the nanoparticles before coating was characterized by scanning electron microscopy (SEM). The nanoparticles were mounted on aluminum stubs, sputter-coated with a thin layer of Au/Pd and examined using an SEM (Seron Technology 2008, Korea).

### Coating the Nanoparticles with Chitosan

The nanoparticles were separated from the dispersion by centrifuging (Microcentrifuge Sigma 30k, UK) at 7000 rpm for 10 min. Different concentrations of chitosan (0.2, 0.4, 0.6% w/v) were prepared in an aqueous solution of 2% v/v of acetic acid. Chitosan solutions were then added to the nanoparticles and subsequently resuspended by vortexing and then incubate at 25°C for 2 h.

### Fourier Transform Infrared Spectroscopy

The Fourier transform infrared (FTIR) spectra of nanoparticles before and after coating with chitosan were taken by FTIR spectrometer (RAYLEIGH, WQF-510/520, China) at wave numbers 500–4000  $\text{cm}^{-1}$  with a resolution of 4  $\text{cm}^{-1}$  using the KBr disc method to confirm the presence of the chitosan coating on the nanoparticles.

### Evaluation of Drug Encapsulation

The drug-loaded nanoparticles before and after coating with chitosan were separated from non-entrapped drug by centrifugation at 10,000 rpm for 10 min at 25°C. The amount of free drug in the clear supernatant was measured using UV spectrometry (RF-5301 PC, Shimadzu, Kyoto, Japan) at 248 nm. The percent of encapsulation efficiency (EE%) of the nanoparticles was calculated according to the following equation:

$$EE\% = \frac{\text{Drug}_{\text{total}} - \text{Drug}_{\text{filtrate}}}{\text{Drug}_{\text{total}}} \times 100 \quad (1)$$

### Particle Size and Zeta Potential Analysis of Nanoparticles

The mean particle diameter of nanoparticles was estimated by photon correlation spectroscopy at a fixed angle of 90°. Samples were diluted with dust free water to give the recommended scattering intensity of 100,000 counts  $\text{s}^{-1}$ , each value is mean of five measurement of 120 s each, divided into ten sub-runs. The diameter was calculated from auto correlation function of intensity of light scattered from particles, assuming a spherical form for particles.

The particle charge was quantified as zeta potential by laser Doppler anemometry using a Malvern Zetasizer 3000 (Zetasizer 3000 HS, Malvern Instrument, UK). Samples were diluted with distilled water. Zeta potential was calculated from the mean electrophoretic mobility.

### In Vitro Drug Release Studies

Phosphate-buffered saline (PBS, pH 7.4), or HCl 0.1N (pH 1.2) containing 2% of Tween 20 was used as the release medium for *in vitro* carvedilol release from the nanoparticles. An amount of 1 mL of nanoparticle dispersion was transferred into a dialysis

bag (cutoff 12 kDa) and placed into a beaker containing 65 mL of PBS. The beaker was then placed in a 37°C water bath and stirred at 100 rpm. At predetermined time intervals, 1 mL samples were withdrawn from the incubation medium and analyzed for the drug content by UV spectrophotometry at  $\lambda_{\text{max}} = 255$  nm for pH 7.4 and at  $\lambda_{\text{max}} = 250.5$  nm for HCl medium. The drug release tests were performed in triplicate.

#### Mucoadhesive Studies

Briefly, a 1 mg mL<sup>-1</sup> solution of mucin was prepared in acetate buffer (pH 4.5) which was then filtered with Whatman no. 1 filter paper. The adsorption-association of mucin on/with the particles was used as a method to assess mucoadhesive properties of the prepared particles. For this purpose, determined volume of nanoparticles dispersion (containing 20 mg mL<sup>-1</sup>) and the solution of mucin were mixed, vortexed, and shaken at 37°C temperature for 3 h. Then the dispersion was centrifuged for 30 min at 10,000 rpm and the free mucin in the supernatant was determined by addition of 200  $\mu$ L of Bradford reagent to 800  $\mu$ L of the dispersion. The samples were incubated at 37°C for 20 min and the concentration of free mucin was measured spectrophotometrically at 595 nm using the standard calibration curve.

#### Preparation of Bradford Reagent

Coomassie Brilliant Blue G-250 (100 mg) was dissolved in 50 mL of 95% ethanol. An amount of 100 mL of 85% (w/v) phosphoric acid was added to this solution. The resulting solution was diluted with water to a final volume of 1 L.

#### Calibration Curve for Measurement of Mucin

A calibration curve was prepared for measurement of mucin by measuring the absorbance of mucin standard solutions 0.1, 0.2, 0.3, 0.4, 0.5 mg mL<sup>-1</sup> in deionized water after adding Bradford reagent.<sup>18</sup> The samples were measured spectrophotometrically at 595 nm.

#### Spray Drying of Carvedilol Loaded in Chitosan-Coated Nanoparticles

A quantity of chitosan-coated nanoparticles equivalent to 50 mg of carvedilol was dispersed separately in 200 mL of PBS containing 20 mg mL<sup>-1</sup> of carrier powder (lactose/Mannitol). Dispersions were spray dried using a spray-dryer (SD-O5, Labplant, England) with pneumatic atomizer through a 1.4 mm nozzle. The spray drying was performed using feed pump rate of 10.0 mL min<sup>-1</sup>, 50% aspiration, inlet temperature of 100  $\pm$  5°C with an outlet temperature of 60–65°C.

#### Solid-State Characterization

Flow properties of the spray-dried powders were determined using angle of repose and Carr's compressibility index. Carr's compressibility index was determined from the tapped and bulk density of spray-dried powders using eq. (2).<sup>19</sup> Tapped density was determined using 10 g of the sample after 100 mechanical taps in a measuring cylinder. The angle of repose was calculated as reported earlier.<sup>20</sup> Hausner ratio was determined from tapped density and bulk density calculated by eq. (3).<sup>21</sup>

$$\text{Carr Index} = [1 - V_b/V_t] \times 100 \quad (2)$$

where  $V_b$  is freely volume of powder,  $V_t$  is tapped volume of the same mass.

$$\text{Hausner ratio} = \rho_T/\rho_B \quad (3)$$

where  $\rho_T$  is tapped bulk density of powder and  $\rho_B$  is freely bulk density of powder.

#### Particle Size Measurement

The particle size distribution of the spray-dried samples was determined by laser diffraction using a Nanozetaser Malvern Mastersizer (Zetasizer 3000 HS, Malvern Instrument, UK). For this purpose, about 5 mg of each spray-dried powder was dispersed in 5 mL of isopropyl alcohol and sonicated for 2 min and the particle size was measured in triplicate.

#### In Vitro Deposition Studies Using Next Generation Impactor

The powders were aerosolized using a dry powder inhalation device (Easy haler). The *in vitro* deposition of the aerosolized drug was investigated using Next Generation Impactor (NGI, Model 170, Apparatus E; British Pharmacopoeia, 2010, USA). A total of 10 mg of each spray-dried powder was loaded into hard gelatin capsules (size 3). An air stream of 60 L min<sup>-1</sup> was produced throughout the system by attaching the outlet of the using NGI to a vacuum pump for 4 s. The powder deposited in Stages 1 to 8, the mouthpiece and the pre-separator device were collected by rinsing with concentrated HCl 0.1N solution and the drug was extracted by chloroform. The drug contents were then determined spectrophotometrically at  $\lambda = 283.5$  nm. From drug deposition data the fine particle fraction (FPF), aerodynamic diameter ( $d_{\text{aer}}$ ), and percentage of emitted dose were calculated. CITDAS Version 3.10, data processing software (Copley Scientific, Nottingham, UK) was used for determination of these parameters.

## RESULT AND DISCUSSION

#### Physicochemical Properties of Carvedilol-Loaded Nanoparticles of PEVA

Table I summarizes the physicochemical properties of carvedilol-loaded nanoparticles before and after coating with chitosan.

The presence of chitosan layer after coating the nanoparticles was shown by comparing the FTIR spectra of nanoparticles before and after coating with chitosan (Figure 1). As seen in Figure 1a the nanoparticles that before coating contained PEVA, PEG, and carvedilol show the typical peaks of these components as follows: the peak at 2920 cm<sup>-1</sup> relates to the amine stretching band of carvedilol, the peak at 3381 cm<sup>-1</sup> relates to the hydroxyl groups of both carvedilol and PEG, the two peaks at 1217 and 1039 cm<sup>-1</sup> also refer to the alkyl aryl ether stretching band vibration of carvedilol, the peak at 1739 cm<sup>-1</sup> indicates the esteric C=O group of PEVA, CH<sub>2</sub> groups of PEG show a peak at 2852 cm<sup>-1</sup> and at last the C–O–C band of PEG shows a peak at 1252 cm<sup>-1</sup>. In Figure 1b broadening of the peak at 3379 cm<sup>-1</sup> relates to the NH symmetric vibration of chitosan and the formation of hydrogen bond between OH groups of PEG and carvedilol. The addition of a peak at 1576 cm<sup>-1</sup> which relates to the stretching vibration of type I amine of chitosan indicates the presence of chitosan on the surface of nanoparticles (Figure 1b). Another reasons for addition of the chitosan coating on the nanoparticles are the presence of peak at 1055 cm<sup>-1</sup> relating to the C–N stretching of type I amine of chitosan

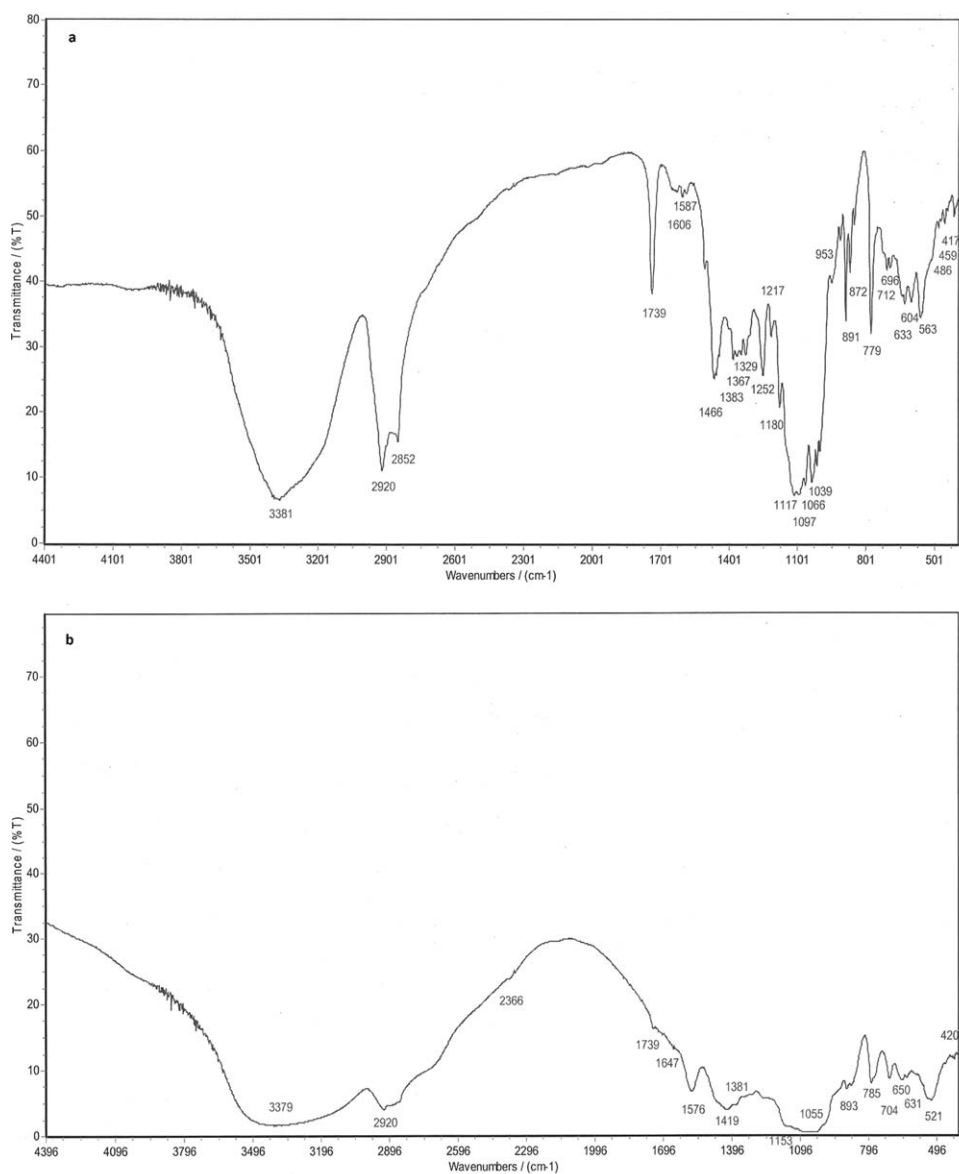
**Table I.** Physicochemical Properties of Carvedilol-Loaded Nanoparticles

Formulations	Particle size (nm)	Zeta potential (mv)	PDI	Drug encapsulation efficiency %
Un-coated nanoparticles	215.2 ± 1.1	5.9 ± 5.5	0.2 ± 0.0	87.9 ± 0.2
Chitosan coated 0.2%	530.5 ± 18.7	39.2 ± 4.9	0.5 ± 0.5	87.5 ± 7.6
Chitosan coated 0.4%	1546.5 ± 408.0	43.1 ± 5.5	0.9 ± 0.2	86.5 ± 5.1
Chitosan coated 0.6%	2223.0 ± 332.3	37.7 ± 19.1	1.0 ± 0.0	87.4 ± 4.1

(Figure 1b) which were absent in Figure 1a (before coating) and also the peak at  $1153\text{ cm}^{-1}$  which indicates the addition of the saccharide structure of chitosan to the nanoparticles.

Carvedilol is a lipophilic molecule. The logarithmic value of the partition coefficient of carvedilol ( $\log P$ ) was found to be  $2.79 \pm 0.03$  (17). High lipophilicity of carvedilol resulted in high entrapment efficiency of this drug in PEVA nanoparticles which them-

selves are composed of a high lipophilic copolymer. There was no significant difference in encapsulation efficiency (EE%) values of different formulations before and after coating with chitosan (Table I). The size of nanoparticles before surface modification was 215.17 nm and was increased after coating them with chitosan (Table I). The chitosan-coated nanoparticles with the highest chitosan concentration had significantly larger mean diameters

**Figure 1.** FTIR spectra of nanoparticles (a) before and (b) after coating with chitosan.



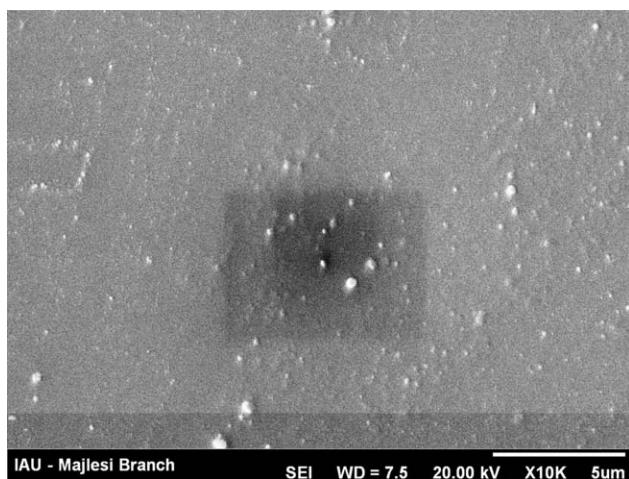


Figure 2. SEM micrographs of nanoparticles of PEVA.

compared to other formulations ( $P < 0.05$ ). This result is in agreement with previous reports showing that an increment in the concentration of chitosan solution caused in nanoparticles size growth.<sup>22,23</sup>

As previously demonstrated drug-loaded chitosan particles have positive surface charge. The results of Table I show that zeta potential of chitosan-coated nanoparticles have significant difference with uncoated nanoparticles ( $P < 0.05$ ) but there is no significant differences in zeta potential of different concentrations of chitosan-coated nanoparticles. Zeta potential of the particles increased upon chitosan coating, which further confirms that the coat of chitosan is deposited on the nanoparticles. Similar result was reported earlier for chitosan-coated liposomes<sup>22–24</sup> and chitosan-coated PLGA microparticles.<sup>18</sup> The formation of coating chitosan layer on surface of nanoparticles might not be the only reason for size increment, but it could be due to agglomeration of nanoparticles.<sup>25</sup> The polydispersity index (PDI) is a measure of dispersion homogeneity and ranges from 0 to 1. Values close to 0 indicate a homogeneous dispersion. In present study the PDI varies in different formulations. Homogeneity of nanoparticles was markedly decreased upon chitosan coating. The nanoparticles with the highest chitosan concentration had significantly highest PDI. High PDI value

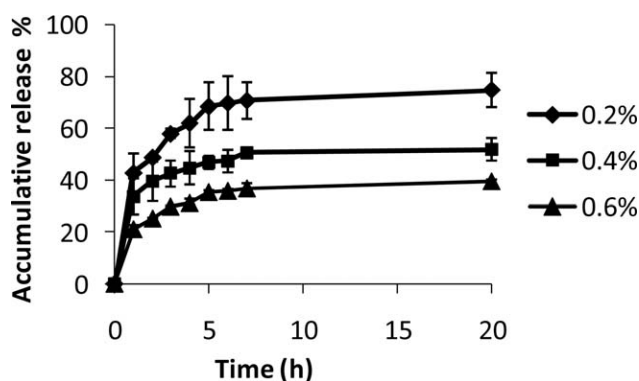


Figure 3. Release profiles of carvedilol from nanoparticles of PEVA coated with different concentrations of chitosan ( $n = 3$ ).

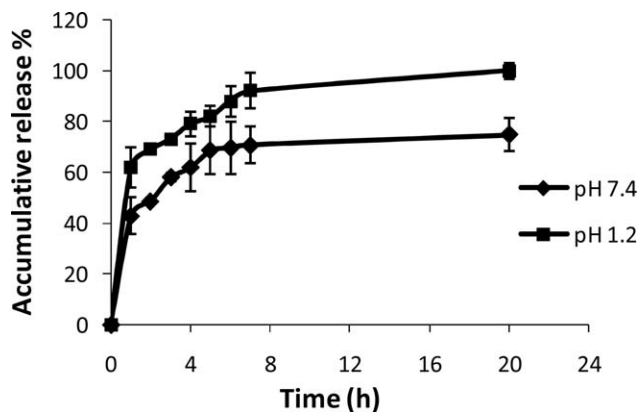


Figure 4. Effect of pH on carvedilol release from nanoparticles of PEVA coated with 0.2% of chitosan ( $n = 3$ ).

indicates a heterogeneous particle size range distribution in the system.

SEM micrographs (Figure 2) show spherical morphology for PEVA nanoparticles. The particle size of nanoparticles seen in SEM is in accordance with DLS method reported in Table I.

#### In Vitro Drug Release Study

The release profiles of carvedilol from the chitosan-coated nanoparticles are presented in Figure 3. As this figure shows drug was released from chitosan-coated nanoparticles in a biphasical model with an initial fast rate followed by a slower one. This faster release could be due to the burst release of carvedilol loaded near the particles surface. Also with increasing the concentration of chitosan the burst release and overall release of drug from nanoparticles reduced. The nanoparticles coated with the lowest amounts of chitosan (0.2%) the release of carvedilol was faster. In fact, the addition of chitosan resulted in marked decrease of carvedilol release, indicating the higher stability of the drug by the addition of chitosan to nanoparticles. Similar result obtained after chitosan coating on rifampicin loaded PLGA microparticles.<sup>26</sup>

To show the effect of pH on the release of carvedilol from PEVA nanoparticles coated with 0.2% of chitosan was studied

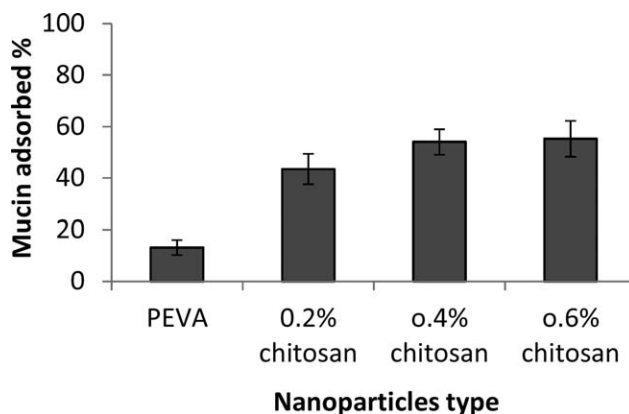


Figure 5. Mucoadhesion of PEVA nanoparticles coated with different concentrations of chitosan ( $n = 3$ ).

**Table II.** The Physical Properties of Inhaler Spray-Dried Powders of Chitosan-Coated Nanoparticles of Carvedilol Using Different Carriers

Carrier type	Particle size ( $\mu\text{m}$ )	Tapped density ( $\text{g}/\text{cm}^3$ )	Bulk density ( $\text{g}/\text{cm}^3$ )	Angle of repose ( $^\circ$ )	Carr's Index	Hausner ratio
Mannitol	$4.2 \pm 0.1$	$0.44 \pm 0.01$	$0.39 \pm 0.02$	$32.3 \pm 0.4$	$12.1 \pm 1.3$	$1.1 \pm 0.0$
Lactose	$3.1 \pm 0.1$	$0.57 \pm 0.02$	$0.46 \pm 0.07$	$34.1 \pm 2.3$	$18.5 \pm 3.2$	$1.2 \pm 0.0$

in two pH. Figure 4 shows faster drug release in acidic pH which is due to the protonation of amino groups of chitosan in this pH which cause hydration of the coating layer and faster drug release while they are deprotonated in PBS (pH 7.4) and a double layered hard nanospheres are formed. The structure of particles coated with chitosan is loose when the  $\text{pH} < \text{pKa}$  of chitosan and becomes compact when  $\text{pH} > \text{pKa}$  of chitosan. This effect indicates a pH sensitive behavior for these nanoparticles. Yao et al.<sup>27</sup> also reported a pH-sensitive behavior for the swelling of a chitosan–pectin polyelectrolyte complex.

#### Mucoadhesive Properties of Carvedilol-Loaded Nanoparticles

The Bradford colorimetric method was used to determine free mucin concentration in order to assess the amount of mucin adsorbed on the nanoparticles. Mucin calibration curve showed a linear relationship between 100 and 500  $\mu\text{g ml}^{-1}$  concentrations with the equation of  $y = 0.0011x + 0.0525$  and regression coefficient of 0.9921. Mucoadhesive properties of carvedilol-loaded nanoparticles were evaluated by measuring mucin adsorption on the particles. From the results presented in Figure 5, nanoparticles coated with chitosan have good mucoadhesive properties as demonstrated by the high amounts of particle associated mucin; while on the contrary, PEVA nanoparticles showed dramatic lower amounts of adsorbed mucin on their surface. Also a direct correlation was observed between the percentage of mucin adsorbed on the nanoparticles and their corresponding zeta potential values (Table I). As much as the coating concentration was increased, the mucoadhesion also grew. This result is in agreement with previous results reported by Zaru et al.<sup>24</sup> who used chitosan-coated liposomes for drug delivery to lungs.

Coated nanoparticles with 0.2% of chitosan were selected as the best formulation due to their acceptable mucoadhesion, nano range particle size and narrow size distribution. These nanoparticles also showed the highest drug release that makes them an appropriate candidate for pulmonary delivery as a drug powder inhalation. These nanoparticles were used for preparation of inhaler powder with spray drying technique using two types of carriers, i.e., lactose and mannitol. The effective inhalation performance of dry-powder products is dependent on the drug formulation and the inhaler device. Dry powder formulations are usually prepared by mixing the micronized drug particles with larger carrier particles. The aerosolization efficiency of a powder is highly dependent on the carrier characteristics, such as particle size distribution, shape, and surface properties. The main objective in the inhalation field is to achieve reproducible, high pulmonary deposition. This could be achieved by successful carrier selection and careful process optimization.<sup>28</sup>

#### Solid-State Characterization of Spray Dried Nanoparticles

The physical properties of the two types of dry powder formulations for inhalation are summarized in Table II.

In order to promote the systemic absorption of the drug, aerosol particles need to reach the alveolar region of the lungs and therefore the proper particle size following dispersion, is between 3 and 5  $\mu\text{m}$ .<sup>29</sup> In present study both spray-dried powders of mannitol and lactose had adequate particle size for inhalation (Table II).

The bulk and tapped density values were obtained for the spray-dried powders. The tap density of each material can be used to predict both its flow properties and respirable fraction. Decreasing the tap density of the dry powders significantly increase the respirable fraction.<sup>1</sup> The Carr's Index, Hausner ratio, and angle of repose generally considered as appropriate criteria for evaluation of the flow properties of solids were also determined.<sup>21</sup> Mannitol spray-dried powder, showed relatively low density characteristics with interesting flow properties but lactose carrier showed intermediate flow properties with relatively higher density. It was observed that mannitol spray-dried powder also had higher process yields because of the lower stickiness to the inner surface of the wall of spray drier cyclone (data were not shown).

#### In Vitro Deposition Studies Using Next Generation Impactor

The pulmonary deposition of the spray-dried powders was investigated *in vitro* using NGI. Influence of the carrier on dry powders FPF, emitted dose percent (ED%), and the aerodynamic diameter ( $d_{\text{aer}}$ ) are summarized in Table III.

Deposition data for different powders after aerosolization of the samples at 60  $\text{L min}^{-1}$  through an Easyhaler®, using NGI, are presented in Figure 6.

As Figure 6 indicates the amounts of drug deposited on various stages of the NGI varied for different samples. This result suggests the different aerodynamic properties of the aerosolized nanoparticles in spray-dried samples. The highest FPF was observed for mannitol spray-dried powder while lactose powder showed the lowest deposition in the lower stage of NGI probably due to the cohesion of individual particles to form larger aggregates and presence of agglomerated particles in the air stream during inspiration through an inhaler.<sup>30</sup> Differences in hygroscopicity of the materials and thereby alteration of capillary forces and/or differences in surface properties may explain those results. Also it has been shown that mannitol has less

**Table III.** Influence of the Carrier on Dry Powders FPF, Emitted Dose, and Aerodynamic Diameter of Spray-Dried Nanoparticles

Carrier type	Emitted dose%	FPF%	$d_{\text{aer}}$ ( $\mu\text{m}$ )
Mannitol	90.49	58.82	1.4
Lactose	90.69	21.26	2.82

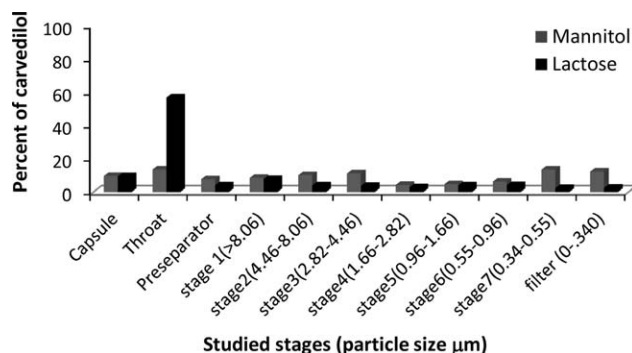


**Figure 6.** Drug deposition patterns of spray-dried nanoparticles of PEVA-loading carvedilol and coated with 0.2% of chitosan with different carriers in the NGI.

large particles aggregate and can be successfully inspired in to lung.<sup>31</sup> However, as Table III shows significant difference was not seen in the emitted dose percent between the different studied of powders ( $P > 0.05$ ). Both the powders exhibited an aerodynamic diameter of individual particles suitable for deep lung deposition, i.e.,  $<3 \mu\text{m}$ . Lower tap density of mannitol (Table II) as well as its less aerodynamic diameter of individual particles significantly increased the respirable fraction of this powder as seen in Figure 6. Drug deposition in the lung is mainly controlled by its aerodynamic diameter.<sup>32</sup> Particles larger than  $5 \mu\text{m}$  are mostly trapped by oropharyngeal deposition and incapable of reaching the lungs while smaller than  $1 \mu\text{m}$  are mostly exhaled without deposition.<sup>33</sup> Particles with aerodynamic diameters between 1 and  $5 \mu\text{m}$  are expected to efficiently deposit in the lung periphery.<sup>34</sup>

## CONCLUSION

Mucoadhesive nanoparticles of PEVA-containing carvedilol can be prepared by solvent evaporation technique and further coating by 0.2% of chitosan. The results of our study allow concluding that mannitol spray-dried nanoparticles are suitable inhaler powder for pulmonary delivery of carvedilol. Further *in vivo* studies are needed to conclude the pharmacokinetic properties of the proposed formulation in comparison with oral dosage forms of carvedilol in its bioavailability enhancement.

## ACKNOWLEDGMENTS

Financial support of this work by Research Vice Chancellor of Isfahan University of Medical Sciences through project No. 191016 is acknowledged.

## REFERENCES

1. Bosquillon, C.; Lombry, C.; Preat, V.; Vanbever, R. *J. Control. Rel.* **2001**, *70*, 329.
2. Venishetty, V. K.; Chede, R.; Komuravelli, R.; Adepur, L.; Sistla, R.; Diwan, P. V. *Colloids Surf. B: Biointerf.* **2012**, *95*, 1.
3. Mahmoud, E. A.; Bendas, E. R.; Mohamed, M. I. *AAPS PharmSciTech.* **2009**, *10*, 183.

4. Patil, S.; Babbar, A.; Mathur, R.; Mishra, A.; Sawant, K. *J. Drug Target.* **2010**, *18*, 321.
5. Mansour, H. M.; Rhee, Y. S.; Wu, X. *Int. J. Nanomed.* **2009**, *4*, 299.
6. Andrade, F.; Goycoolea, F.; Chiappetta, D. A.; das Neves, J.; Sosnik, A.; Sarmiento, B. *Int. J. Carbohydr. Chem.* **2011**, Article ID 865704.
7. Thanou, M.; Verhoef, J. C.; Junginger, H. E. *Adv. Drug Deliv. Rev.* **2001**, *50*, 91.
8. Cypesa, S. H.; Saltzman, W. M.; Giannelis, E. P. *J. Control. Rel.* **2003**, *90*, 163.
9. Park, J. H.; Cho, Y. W.; Cho, Y. H.; Choi, J. M.; Shin, H. J.; Bae, Y. H.; Chung, H.; Jeong, S. Y.; Kwon, I. C. *J. Biomater. Sci. Polym. Ed.* **2003**, *14*, 951.
10. Lee, W. L.; Widjaja, E.; Loo, S. C. *Small* **2010**, *6*, 1003.
11. de Queiroz, A. A.; Abraham, G. A.; Higa, O. Z. *Acta Biomater.* **2006**, *2*, 641.
12. Keskar, V.; Mohanty, P. S.; Gemeinhart, E. J.; Gemeinhart, R. A. *J. Control. Rel.* **2006**, *115*, 280.
13. Beeley, N. R. F.; Stewart, J. M.; Tano, R.; Lawin, L. R.; Chappa, R. A.; Qiu, G.; Anderson, A. B.; de Juan, E.; Varner, S. E. *J. Biomed. Mater. Res.* **2006**, *76A*, 690.
14. Tallury, P.; Alimohammadi, N.; Kalachandra, S. *Dent. Mater.* **2007**, *23*, 404.
15. Shin, S. C.; Lee, H. J. *Eur. Pharm. Biopharm.* **2002**, *54*, 201.
16. Vasudev, S. C.; Chandy, T.; Sharma, C. P. *Biomaterilas* **1997**, *18*, 375.
17. Thimmasetty, J.; Pandey, G. S.; Sathesh Babu P. R. *Pak. J. Pharm. Sci.* **2008**, *21*, 241.
18. Manca, M. L.; Mourtas, S.; Dracopoulos, V.; Fadda, A. M.; Antimisiaris, S. G. *Colloids Surf. B: Biointerf.* **2008**, *62*, 220.
19. Chougule, M.; Padhi, B.; Misra, A. *AAPS PharmSciTech.* **2008**, *9*, 47–53.
20. Shah, S. P.; Misra, A. *AAPS PharmSciTech.* **2004**, *5*, 107–113.
21. Ahmad, M. Z.; Akhter, S.; Ahmad, I.; Singh, A.; Anwar, M.; Shamim, M.; Ahmad, F. J. *Expert Opin. Drug Deliv.* **2012**, *9*, 141.
22. Guo, J.; Ping, Q.; Jiang, G.; Huang, L.; Tong, Y. *Int. J. Pharm.* **2003**, *260*, 167.
23. Zhuang, J.; Ping, Q.; Song, Y.; Qi, J.; Cui, Z. *Int. J. Nanomed.* **2010**, *5*, 407.
24. Zaru, M.; Manca, M. L.; Fadda, A. M.; Antimisiaris, S. G. *Colloids Surf. B: Biointerf.* **2009**, *71*, 88.
25. Karn, P. R.; Vanić, Z.; Pepić, I.; Škalco-Basnet, N. *Drug Dev. Ind. Pharm.* **2011**, *37*, 482.
26. Manca, M. L.; Loy, G.; Zaru, M.; Fadda, A. M.; Antimisiaris, S. G. *Colloids Surf. B: Biointerf.* **2008**, *67*, 166.
27. Yao, K. D.; Tu, H.; Cheng, F.; Zhang, J. W.; Liu, J. *Macromol. Mater. Eng.* **1997**, *245*, 63.
28. Rahimpour, Y.; Hamishehkar, H. *Adv. Pharm. Bull.* **2012**, *2*, 183.
29. Vidgren, M. T.; Vidgren, P. A.; Paronen, T. P. *Int. J. Pharm.* **1987**, *35*, 139.

30. Pilcer, G.; Wauthoz, N.; Amighi, K. *Adv. Drug Deliv. Rev.* **2012**, *64*, 233.
31. Vanbever, R.; Mintzes, J. D.; Wang, J.; Nice, J.; Chen D.; Batycky, R.; Langer, R.; Edwards, D. A. *Pharm. Res.* **1999**, *16*, 1735.
32. Wolff, R. K.; Dorato, M. A. *Crit. Rev. Toxicol.* **1993**, *23*, 343.
33. Sakagami, M. *Adv. Drug Deliv. Rev.* **2006**, *58*, 1030.
34. Heyder, J.; Gebhart, J.; Rudolf, G.; Schiller, C. F.; Stahlhofen, W. *J Aerosol. Sci.* **1986**, *17*, 811.